Nitric Oxide 87 (2019) 73–82

Contents lists available at ScienceDirect

Nitric Oxide

journal homepage: www.elsevier.com/locate/yniox

Exercise training augments neuronal nitric oxide synthase dimerization in the paraventricular nucleus of rats with chronic heart failure

Neeru M. Sharma*, Xuefei Liu, Tamra L. Llewellyn, Kenichi Katsurada, Kaushik P. Patel

Department of Cellular and Integrative Physiology, UNMC, Omaha, NE 68198-5850, USA

ARTICLE INFO

Keywords:
nNOS
PIN
BH4
Exercise training
Paraventricular nucleus

ABSTRACT

Exercise training (ExT) is an established non-pharmacological therapy that improves the health and quality of life in patients with chronic heart failure (CHF). Exaggerated sympathetic drive characterizes CHF due to an imbalance of the autonomic nervous system. Neuronal nitric oxide synthase (nNOS) in the paraventricular nucleus (PVN) produce nitric oxide (NO•), which is known to regulate the sympathetic tone. Previously we have shown that during CHF, the catalytically active dimeric form of nNOS is significantly decreased with a concurrent increase in protein inhibitor of nNOS (PIN) expression, a protein that dissociates dimeric nNOS to monomers and facilitates its degradation. Dimerization of nNOS also requires (6R)-5,6,7,8-tetrahydrobiopterin (BH4) for stability and activity. Previously, we have shown that ExT improves NO-mediated sympathetic inhibition in the PVN; however, the molecular mechanism remains elusive. We hypothesized; ExT restores the sympathetic drive by increasing the levels and catalytically active form of nNOS by abrogating changes in the PIN in the PVN of CHF rats. CHF was induced in adult male Sprague-Dawley rats by coronary artery ligation, which reliably mimics CHF in patients with myocardial infarction. After 4 weeks of surgery, Sham and CHF rats were subjected to 3 weeks of progressive treadmill exercise. ExT significantly ($p < 0.05$) decreased PIN expression and increased dimer/monomer ratio of nNOS in the PVN of rats with CHF. Moreover, we found decreased GTP cyclohydrolase 1(GCH1) expression: a rate-limiting enzyme for BH4 biosynthesis in the PVN of CHF rats suggesting that perhaps reduced BH4 availability may also contribute to decreased nNOS dimers. Interestingly, CHF induced decrease in GCH1 expression was increased with ExT. Our findings revealed that ExT rectified decreased PIN and GCH1 expression and increased dimer/monomer ratio of nNOS in the PVN, which may lead to increase NO• bioavailability resulting in amelioration of activated sympathetic drive during CHF.

1. Introduction

A hallmark of chronic heart failure(CHF) is increased neurohumoral drive and overactivation of the renin-angiotensin system and sympathetic nervous system [1]. Enhanced sympathetic signaling exacerbates cardiac stress, both directly and by stimulating fluid retention by the kidneys through increased renal sympathetic nerve activity (RSNA) which is an important cause of morbidity and mortality despite significant improvements in the treatment. Exercise training (ExT) is an established non-pharmacological therapy that improves the health and quality of life in patients with CHF. According to the recently launched American Heart Association guidelines for Overall Cardiovascular Health, there is a recommendation of moderate-intensity aerobic activity for 30 min at least five days per week and for lowering blood pressure and cholesterol an average 40 min of moderate-to vigorous-intensity aerobic activity 3 or 4 times per week [2].

The paraventricular nucleus (PVN) of the hypothalamus, a key area that integrates sympathetic outflow, is activated in CHF [3–8]. PVN contains preautonomic neurons that affect sympathetic outflow either directly by projections to the intermediolateral cell column in the spinal cord or via the rostral ventrolateral medulla and also reciprocally connected to other areas of the brain involved in the control of cardiovascular function [3,9–11]. A number of different neurotransmitters converge to influence the PVN neuronal activity [3,12,13] and altered inhibitory (nitric oxide/GABA) and excitatory (glutamate/angiotensin II) mechanisms within the PVN induce exaggerated sympathetic excitatory responses in pathological conditions such as hypertension and CHF [6,14,15]. In the PVN, nitric oxide (NO•) acts as a retrograde inhibitory neurotransmitter that regulates synaptic efficacy and modulates neuronal activity and has also been suggested to play an essential role in the regulation of sympathetic outflow [16,17] leading to changes in sympathetic nerve activity. Decrease levels of NO• reduced GABA released and its inhibitory actions [18] and enhanced the

* Corresponding author. Department of Cellular and Integrative Physiology, University of Nebraska Medical Center, 985850 Nebraska Medical Center, Omaha, NE 68198-5850, USA.
E-mail address: nsharma@unmc.edu (N.M. Sharma).

https://doi.org/10.1016/j.niox.2019.03.005
Received 17 July 2018; Received in revised form 6 February 2019; Accepted 8 March 2019
Available online 13 March 2019
1089-8603/

glutamatergic actions observed in rats with CHF [19].

Previously, we reported that ExT improves endogenous blunted NO•, mechanisms within the PVN in rats with heart failure [20]. The regulatory details and the possible mechanism(s) of this phenomenon remain largely unknown. In our recent studies, we demonstrated the protein inhibitor of neuronal nitric oxide synthase (nNOS) abbreviated as a PIN-mediated posttranslational mechanism affecting the nNOS levels within the PVN of rats with CHF [21]. The PIN was reported to bind to a 17-residue peptide fragment from Met-228 to His-244 of nNOS [22] and destabilize nNOS dimers [23], a conformation required for activity of the enzyme [24]. The ubiquitin-proteasome system degrades the functionally impeded monomeric enzyme. Our work demonstrated that the downregulation of nNOS in the PVN during CHF is due to the ubiquitin-mediated proteolytic degradation involving interactions between nNOS and PIN through an Ang II-mediated signaling pathway(s). The diminished levels of dimeric nNOS may lead to decrease NO•-mediated sympathoinhibition. This study was conducted to determine if ExT restores the dimeric nNOS levels by decreasing the levels of the PIN in the PVN of rats with CHF.

2. Methods

2.1. An animal model of congestive heart failure

Male Sprague-Dawley rats weighing 220–240 g were purchased from Sasco Breeding Laboratories, Omaha, NE. Rats were housed at room temperature (24–26 °C) in a 12-h light-dark cycle room and given free access to food and water according to approved guidelines of the University of Nebraska Medical Center, Institutional Animal Care and Use Committee (IACUC). IACUC followed the guidelines suggested in "Guide for the Care and Use of Laboratory Animals" published by the US National Institutes of Health (National Academic Press; 2011). All protocols used for these studies were submitted, reviewed, and approved by the University of Nebraska Medical Center-IACUC committee under the provisions of the Animal Welfare Assurance (A3294-01). CHF was induced by coronary artery ligation as previously described [5,25–27]. Briefly, rats were randomly assigned to two groups: CHF and Sham. Rats were ventilated at a rate of 60 breaths/min with 2–3% isoflurane during the surgical procedure. The left anterior descending coronary artery was ligated between the pulmonary artery outflow tract and the left atrium. Sham-operated rats were prepared in the same manner without coronary artery ligation. The rats were allowed to recover for 4 weeks before experimentation. The left ventricular dysfunction and failure at the end of each experiment (7 weeks) were assessed by hemodynamic and anatomic parameters [28]. Echocardiograms were performed to measure left ventricular end-systolic (LVESD), left ventricular end-diastolic (LVEDD) dimensions, fractional shortening (FS) and ejection fraction (EF). Left ventricular end-diastolic pressure (LVEDP) were measured using a Mikro-Tip catheter (Millar Instruments, Houston, TX) inserted into the left ventricle via the right carotid artery. To measure infarct size, the heart was dissected free of adjacent tissues, atria and the right ventricle were removed and a digital image of the left ventricle was captured using a Kodak DC290 digital camera (Kodak, Rochester, NY). The infarcted area and total left ventricle area were quantified using Sigma Scan Pro. Infarct size (%) was determined by dividing the size of the infarcted area by the total size of the left ventricle. Rats with elevated LVEDP ($\geq$15 mmHg) and infarct size (> 30% of total left ventricle wall) were considered to be in CHF. The rats that did not fit the criteria (listed above) after coronary artery surgery were excluded. The coronary artery ligation-induced heart failure model has been used extensively [5,14,25,26,29] and produces a model of heart failure in the rat similar to the most common cause of human heart failure [25–27].

2.2. Exercise training protocol

Four weeks after ligation surgery, Sham and CHF rats were randomly divided into two groups each subjected to 3 weeks of progressive treadmill exercise. During the training period, rats were exercised between 5 and 15min/day at an initial treadmill speed of 10 m/min to a 0% grade for five days. To ensure a significant endurance ExT regimen, the treadmill grade and speed were gradually increased to 10% and 25 m/min, respectively, and the exercise duration was increased to 60min/day. Only animals that ran steadily on the treadmill with very little or no prompting (electrical stimulation) were included in the study. The remaining Sham and CHF rats were handled daily and treated similar to the ExT rats except for the treadmill running. These animals were referred to as sedentary. Four groups of rats used were the following: 1) Sham-SED; 2) Sham-ExT; 3) CHF-Sed; 4) CHF-ExT.

2.3. Micropunch of the PVN area

The rat was euthanized by pentobarbital (65 mg/kg/ip), the brain was removed and quickly frozen on dry ice. The PVN was punched bilaterally using a diethylpyrocarbonate-treated blunt 18-gauge needle attached to a syringe using Palkovit and Brownstein [30] technique as documented previously [21,26,28,31].

2.4. Western blot analysis

The punched PVN tissues were lysed in lysis buffer (10 mM Tris,1 mM EDTA, 1% SDS, 0.1% Triton X-100 containing complete protease inhibitor cocktail). Equal quantities of protein lysates were separated by 12% sodium dodecyl sulfate-polyacrylamide gel electrophoresis (SDS-PAGE) for PIN(20 μg), and 10% SDS-PAGE for GCH1(30 μg), and nNOS (20 μg), under reducing conditions, and then electrophoretically transferred to a polyvinylidene difluoride(PVDF) membrane (Millipore). Non-fat dry milk (5% w/v) in TBST (10 mM Tris, 150 mM NaCl, 0.05% Tween-20) was used to block membrane at ambient temperature for 1 h. Blots were probed with the antibody directed against PIN (Santa Cruz, sc-13969 [21,32–34],1:500 dilution), nNOS [21,28,32,35,36] (Santa Cruz, sc-302,1:500 dilution), GCH1 [37] (Origene, TA323417, 1:1000 dilution), tubulin(Sigma, T4026, 1:1500 dilution), or β-actin (Santa Cruz, sc-4778,1:2000 dilution). The phosphorylated nNOS Ser ^{847} [38,39] (Abcam, ab-16650,1:1000 dilution), and nNOS Ser ^{1417} [40,41] (Thermo Fisher, PA1-032,1:1000 dilution) in the PVN were detected using 5% BSA as blocking buffer. The membranes were then incubated for 40 min at room temperature with horseradish peroxidase-conjugated corresponding secondary antibodies and finally developed using enhanced chemiluminescence (ECL) reagents (Pierce Chemical, Rockford, IL). Image J (NIH) was used to quantify the signal.

2.5. Determination of SDS-resistant nNOS dimers and monomers

SDS-resistant nNOS dimers and monomers were assayed using low-temperature SDS-PAGE (LT-PAGE) under reducing conditions [42] as described previously [21]. Briefly, 40 μg of protein in standard Laemmli buffer was incubated at 4 °C for 30 min before fractionation using a 5% separating gel. The electrophoresis was done in a cold room at 50 V, and gel and buffers were pre-equilibrated to 4 °C before electrophoresis, to maintain the gel temperature below 15 °C. After LT-PAGE, the gels were transferred to PVDF membrane overnight in cold room at 30 V, and the blots were probed with nNOS antibody as per routine Western blot analysis.

2.6. Immunofluorescence staining

The staining was performed for PIN in coronal brain sections including the PVN from four groups of rats. Anesthetized rats (pentobarbital, 65 mg/kg) were perfused with 150 ml of heparinized saline transcardially followed by 250 ml of 4% paraformaldehyde in 0.1 M sodium phosphate buffer [28]. The brain was post-fixed at 4 °C for 4 h in 4% paraformaldehyde solution and then placed in 30% sucrose for 72 h. The blocking of free-floating sections (30 μm) was performed with 10% normal goat serum, 0.02% Triton X-100 in phosphate buffered saline (PBS) for 1 h at room temperature and then incubated with the PIN (sc-13969, 1:200)

primary antibody overnight. After washing with PBS, the sections were incubated with Cy3-conjugated goat anti-rabbit (1:500) secondary antibody for 4 h at room temperature in the dark. After washing with PBS, the sections were mounted on slides with fluoromount-G (Southern Biotech, AL). Leica-DMR microscope with corresponding filters was used to observe the slides and Image J software (NIH) was used to quantify immunofluorescence. Three alternate sections (2.0 ± 0.2 mm posterior to bregma) representing the PVN were analyzed.

2.7. Tetrahydrobiopterin and dihydrobiopterin ELISA

Tissue level of tetrahydrobiopterin (BH4) and dihydrobiopterin (BH2) was measured in the PVN lysates using ELISA kit from MyBioSource; San Diego, CA following manufacturer instructions in quadruplicate. BH4 ELISA kit utilizes a monoclonal anti-BH4 antibody and a BH4-HRP conjugate, and BH2 ELISA kit has precoated rat BH2 on the solid phase supporter. Spectrophotometric data were measured using a microplate reader at a wavelength of 450 nm. BH4 and BH2 concentration in each sample was interpolated from this standard curve and expressed as pg/μg of PVN protein.

2.8. Renal sympathetic nerve activity (RSNA) recordings

For General surgery for hemodynamic and RSNA measurement, rats were anesthetized with urethane (0.75 g/kg IP) and α-chloralose (70 mg/kg I) and placed in a stereotaxic apparatus (David Kopf Instruments, Tujunga, CA, USA). Body temperature was maintained at 36–38 °C by a heated stage. The trachea was cannulated with polyethylene tubing (PE-240), and the left femoral vein was cannulated with PE-50 for injection of supplemental anesthesia. RSNA was monitored in four groups of rats, as described before [28,43–45]. Briefly, under anesthesia, the left kidney was exposed by a retroperitoneal flank incision. The renal nerve was isolated, placed on a bipolar platinum electrode and secured with a WACKER SilGel mixture (604 and 601). The electrical signal from the electrode was amplified with a Grass amplifier with a high and low-frequency cutoff of 1000 Hz and 100 Hz. The signal was recorded with the PowerLab. The RSNA, recorded at the end of the experiment (after cutting the proximal end) was defined as background noise. The value of basal RSNA was calculated by subtracting the background noise from the actual recorded value. The left femoral artery cannulated with PE-50 was connected via a pressure transducer (Gould P23 1D) to a computer-based data recording and analyzing program (PowerLab) to record mean arterial blood pressure (MAP) and heart rate (HR) by previously established methods [28,44].

2.9. 7-Nitroinidazole (7-NI) microinjection

Anesthetized rats were placed in a stereotaxic apparatus (David Kopf Instruments, Tujunga, CA, USA). For microinjections into the PVN, the bregma was exposed after making a longitudinal incision on the head, and a small burr hole was made in the skull to allow access to the PVN for the placement of microinjection cannulas. The coordinates for the PVN, determined with the Paxinos and Watson atlas, were 1.5 mm posterior to the bregma, 0.4 mm lateral to the midline, and 7.8 mm ventral to the dura. A thin needle (0.2 mm OD) connected to a 0.5 mL microsyringe (Hamilton, Reno, NV, USA) was lowered into the PVN. 7-NI was injected into the PVN in three doses, 50pmol/50 nl, 100pmol/100 nl and 200pmol/200 nl in a random order using the same pipette containing 7-NI. Succeeding injections were made at least 20 min after prior dose to allow MAP, HR, and RSNA to return to basal levels. The peak response of RSNA to the administration of drugs into the PVN during the experiment (averaged over 20–30 s) was subsequently expressed as percent change from baseline.

2.10. Assessment of cardiac function

The LVEDP and rate of change of left ventricular pressure (dP/dt) were evaluated in anesthetized rats before sacrificing or at the time of the terminal experiments after RSNA recordings and 7-NI microinjection into the PVN. Rats were anesthetized with urethane (0.75 g/kg ip) and α-chloralose (70 mg/kg ip), and a Mikro-Tip catheter (Millar Instruments, Houston, TX) containing a pressure transducer was introduced into the left ventricle via the right carotid artery for measurement of LVEDP and dP/dt. A PowerLab data-acquisition system was used for acquiring data.

2.11. Statistical analyses

The data were expressed as mean ± SEM. Analysis of RSNA, MAP and HR was performed by two way repeated measures ANOVA for multiple comparisons. All other results were analyzed by one-way ANOVA followed by Bonferroni's analysis using Prism 7; GraphPad Software. All differences were considered significant at a p-value of < 0.05.

3. Result

3.1. Characteristics of CHF model

Table 1 summarizes the baseline characteristics of the four groups of rats Sham-Sed, CHF-Sed, Sham-ExT, and CHF-ExT utilized in this study. The infarcted area in the CHF group(6–8 weeks after coronary artery ligation) was approximately 34% of the endocardial surface of the left ventricle. Sham rats had no observable damage to the myocardium. LVEDP was significantly increased in the CHF group compared to Sham. dP/dt maximum and minimum were decreased considerably in the CHF group compared to the Sham group, indicating a reduced cardiac contractile and diastolic function. Taken together, the > 30% infarct size, increased LVEDP, and decreased dP/dt suggest that rats in the CHF group were experiencing cardiac dysfunction. LVEDP was significantly

Table 1
Morphological and hemodynamic characteristics of four groups of rats: Sham-SED, Sham-ExT, CHF-Sed, and CHF-ExT.

	Sham-Sed (n = 5)	CHF-Sed (n = 5)	Sham-ExT (n = 5)	CHF-ExT (n = 5
Body weight(g)	404.6 ± 14.2	401.4 ± 15.8	372.4 ± 11.2	359.0 ± 6.9
Infarct size (% of left ventricle)	0	38.2 ± 2.0*	0	31.5 ± 1.8#
LV end-diastolic pressure, (mmHg)	4.5 ± 0.4	29.6 ± 2.5*	4.0 ± 0.8	18.1 ± 3.5#
dP/dt max (mmHg/sec)	9265.2 ± 752.8	4859.4 ± 401.2*	8888.4 ± 383.4	6888.4 ± 572.8#
dP/dt min (mmHg/sec)	−10455.8 ± 560.8	−4117.2 ± 586.0*	−11603.4 ± 477.4	−7798.2 ± 1254.8#
MAP (mmHg)	119.0 ± 3.9	113.8 ± 3.5	123.73 ± 4.8	116.5 ± 4.3
HR (bpm)	371.2 ± 12.7	379.7 ± 5.7	365.2 ± 7.3	348.8 ± 18.0
Citrate synthase activity(îmol/g/min)	11.5 ± 1.5	12.8 ± 0.7	18.2 ± 2.9*	16.3 ± 1.8#

Data are represented as mean ± SE.
LVEDP, left ventricular end-diastolic pressure; dP/dt, left ventricular contractility (delta pressure divided by delta time); MAP, mean arterial pressure; HR, heart rate.
* $P < 0.05$ versus Sham-Sed group.
# $P < 0.05$ versus CHF-Sed group.

high in both CHF-Sed and CHF-ExT rats compared with sham groups and was partially normalized by ExT. While ExT only partially normalized LVEDP, the values in the CHF-ExT group were nonetheless significantly higher from those in either of the sham groups. Furthermore, CHF-Sed rats had a significantly lower change in pressure over time; dP/dt compared with sham rats, which was partially improved by ExT. As documented in our previous studies we have not observed statistically significant differences in basal MAP and HR among the four groups although ExT tended to lower HR in both the sham and CHF groups. Basal RSNA was significantly higher in CHF rats, and ExT reduced the resting basal level of RSNA(Fig. 1A and B). These data confirm that rats in the CHF groups were experiencing cardiac dysfunction and that ExT normalizes cardiac dysfunction per se. Further, we used citrate synthase activity in the soleus muscle, as a metabolic marker in assessing oxidative and respiratory capacity, considering the increased activity of a muscle associated with ExT. In the current study, ExT increased citrate synthase activity in ExT animals (18.2 ± 2.9 μmol/g/min for Sham- ExT and 16.3 ± 1.8 μmol/g/min for CHF− ExT) compared to sedentary animals (11.5 ± 1.5 μmol/g/min Sham-Sed and 12.8 ± 0.7 μmol/g/min, CHF-Sed) demonstrating a significant effect of ExT. The level of citrate synthase activity in the soleus muscle was not significantly different in the Sham-ExT and CH-ExT rats, indicating that comparable level of ExT (moderate level) was performed in both groups of animals(Table 1).

3.2. Central inhibitory NO• mechanism in the PVN in CHF

The catalytically active nNOS dimers [21] and hence NO•-mediated sympathoinhibition is reduced in the PVN of rats with CHF [20,45]. Fig. 2 represents the group data for the changes in RSNA, MAP, and HR obtained by the unilateral microinjection of 7-NI (50, 100, and 200 pmol) into the PVN. 7-NI caused a significant dose-dependent increase in RSNA, MAP, and HR in the sham and CHF groups. However, the increase In RSNA in response to 7-NI in the CHF group was significantly blunted at all three doses compared with Sham (Fig. 2A). At 200 pmol, the changes in RSNA in the CHF group was (9.51 ± 0.78) significantly lower ($p < 0.05$) than in the Sham (17.49 ± 2.53). It should be noted that, although CHF rats tended to have an increased basal RSNA, the absolute increases in RSNA to 7-NI were significantly less in rats with CHF suggesting that that the catalytically active functional dimers are reduced in the PVN during the heart failure condition. A similar trend was observed in MAP (Fig. 2B) and HR (Fig. 2C) responses to 7-NI. The inhibition observed with 7-NI is consistent with a decreased endogenous NO• production in the CHF group because of the inability of nNOS to synthesize NO• as a monomer. Further, we determined the expression of phosphorylated nNOS-Ser^{847} (nNOS-pS^{847}, inhibition of nNOS activity) and phosphorylated nNOS-Ser^{1417} (nNOS-pS^{1417} activation of nNOS activity) in the PVN. The absolute amount of nNOSpS^{847} (0.47 ± 0.09 CHF vs. 0.28 ± 0.04 Sham) as well as ratio of nNOSpS^{847}/total nNOS(1.02 ± 0.15 CHF vs. 0.24 ± 0.03 Sham) was significantly increased in the PVN of CHF rats (Fig. 2D and E) suggesting that there is an increased inactivated pool of nNOS which may decrease in NO• availability. In contrast to this we did not see any changes in the phosphorylation status of nNOS-pS^{1417} in CHF group compared to Sham in absolute amount (0.45 ± 0.05 CHF vs. 0.58 ± 0.09 Sham) and the ratio of nNOSpS^{1417}/total nNOS (0.72 ± 0.10 CHF vs. 0.54 ± 0.11 Sham) (Fig. 2E and F).

3.3. PIN expression is decreased within the PVN after ExT in CHF

Fig. 3A and B shows that there is an increased expression of the PIN in the PVN of CHF rats (0.68 ± 0.10 CHF vs. 0.38 ± 0.07 Sham), and ExT significantly ameliorates this increased expression (0.48 ± 0.05 CHF-ExT vs. 0.68 ± 0.10 CHF). To support the biochemical data, sections of the PVN were immunostained for the PIN *in situ*, in four groups of rats (Fig. 3C). PIN immunostaining increased in the ventromedial parvocellular sub nucleus as well as in the magnocellular portions of the PVN in CHF rats compared to Sham, while ExT reduced the expression of the PIN in CHF-ExT group as represented in cumulative data (Fig. 3D).

3.4. ExT increases BH4 levels via restoring the GCH1 expression within the PVN in CHF

In this experiment, we have examined the levels of BH4, a major cofactor for nNOS activity and NO• synthesis and GCH1, a rate-limiting enzyme in the pathway of BH4 biosynthesis in the PVN lysates. BH4 levels were significantly reduced(~1.41 fold) while oxidized form BH2 were correspondingly increased (~3.5-fold) in the PVN of CHF rats compared to Sham (Fig. 4A and B). Furthermore, the expression of

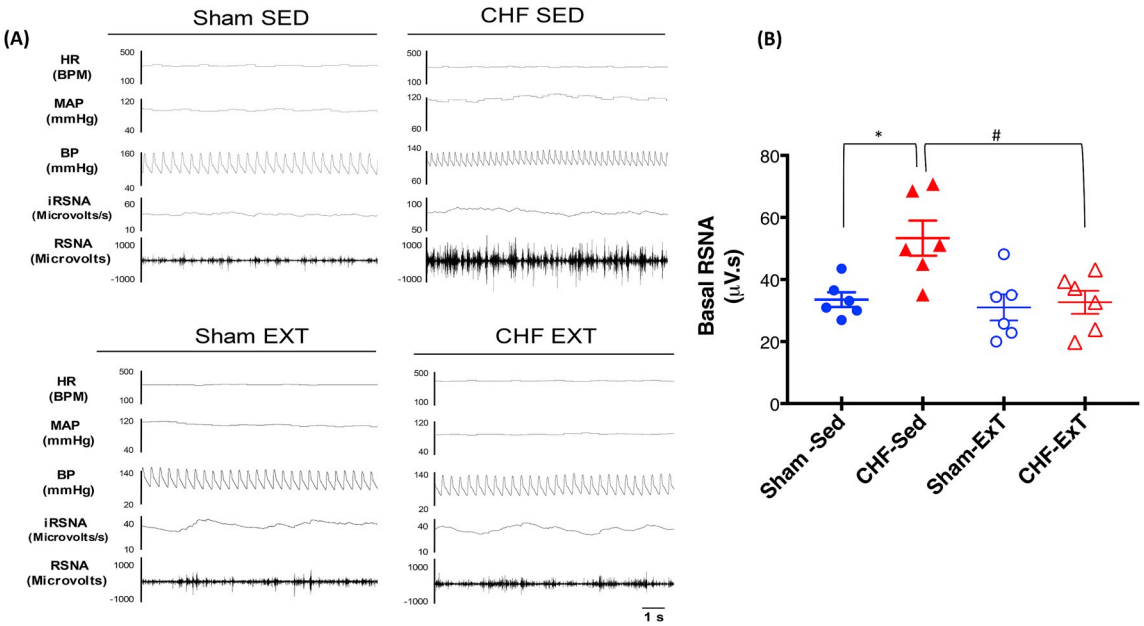

Fig. 1. Baseline Renal sympathetic nerve activity (RSNA), mean arterial pressure (MAP), and heart rate in four groups of rats. (A) segments of original recordings from individual rats from each experimental group (B) mean basal RSNA. *P < 0.05 vs. Sham, #P < 0.05 vs. CHF.

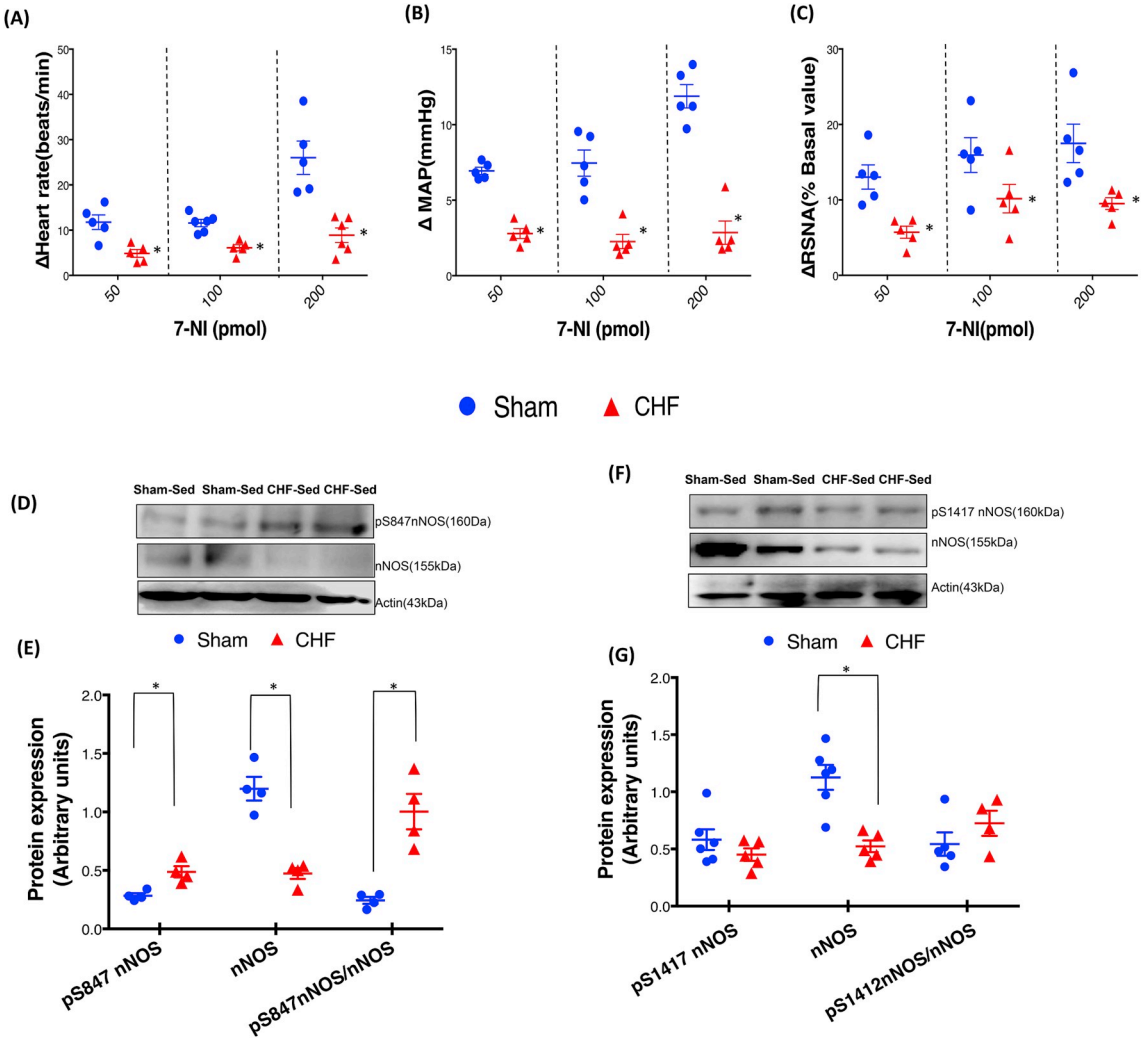

Fig. 2. RSNA, MAP, and HR responses to 7-NI microinjection in the PVN of Sham and CHF rats. (A) mean changes in RSNA, (B) MAP, and (C) HR following microinjections of different doses of 7-NI in the PVN. *P < 0.05 vs. sham with the same dose of 7-NI. Values were mean ± SE from six Independent experiments. Western blot analysis of phosphorylation of nNOS at Ser^{847} and Ser^{1417} in the PVN of Sham and CHF rats. (D, F) Representative Western blot (E, G) densitometry analyses of nNOSpS^{847}and nNOSpS^{1412} normalized to Actin and total nNOS in the PVN. Values are mean SEM (n = 5–6 rats per group) *P < 0.05 vs. Sham.

GCH1 was also reduced in the PVN of CHF rats (0.49 ± 0.03 CHF vs. 0.74 ± 0.06 Sham) (Fig. 4C and D) suggesting that decreased expression of GCH1 limits the availability of BH4 and hence promotes uncoupling of nNOS in the PVN. Interestingly, ExT increases the BH4 content (437.2 ± 24.94 CHF-Sed vs. 577.2 ± 38.21 CHF-ExT, pg/ug protein) as well as GCH1 expression(0.49 ± 0.01 CHF-Sed vs. 0.70 ± 0.05 CHF-ExT) and decreases the BH2 content (3.24 ± 0.43 CHF-Sed vs. 1.40 ± 0.32 CHF-ExT, pg/ug protein) in the PVN (Fig. 4).

3.5. The dimeric form of nNOS levels are increased within the PVN after ExT in CHF

Next, we examined the level of monomeric and dimeric forms of nNOS in PVN lysates using LT-PAGE so that the SDS-resistant dimeric form of nNOS could be measured (Fig. 5A and B). Under normal denaturing conditions, nNOS migrates on SDS-PAGE as a single band of 155 kDa (inactive form), whereas non-boiled tissue homogenates using LT-PAGE separates into a 310-kDa dimer (active form) and a 155-kDa monomer (inactive). The ratio of the dimer and monomer bands determines the relative activity level of nNOS [24]. Consistent with our previous findings [21], we observed a decrease in dimer/monomer ratio of nNOS in rats with CHF (0.67 ± 0.13) compared to Sham rats (1.12 ± 0.04) in the PVN and following ExT, dimer/monomer ratio in CHF group were restored to comparable levels to those in Sham rats (0.89 ± 0.04 CHF-ExT vs. 1.01 ± 0.06 Sham-ExT).

4. Discussion

The novel finding of the present study is that ExT increases the dimeric nNOS in the PVN of rats with CHF via regulating the levels of intracellular factors involved in regulation of nNOS post-translationally. Since ExT was initiated after three weeks of coronary artery ligation, it is likely that ExT is preventing or minimizing rather than reversing the changes in dimeric nNOS in the CHF via changing the availability of these intracellular factors. The PIN is an endogenous inhibitor of nNOS, co-localizes with nNOS in neurons, and also interacts physically with nNOS as demonstrated by our co-immunoprecipitation studies [21]. The function of PIN binding is not fully understood, but it was initially reported to destabilize the nNOS dimer [23] leading to catalytically impaired monomers. In our previous studies, we reported that absolute levels of nNOS [20,28] as well as catalytically active dimeric nNOS expression, is decreased in CHF [21]. The biosynthesis of NO• depends on the availability of the NOS cofactors: viz. reduced flavins, heme iron, BH4, as well as nicotinamide adenine dinucleotide phosphate (NADPH) as an electron source. Homodimerization and cofactor binding is critical for the enzymatic activity of NOS [46] because electrons transfer occurs

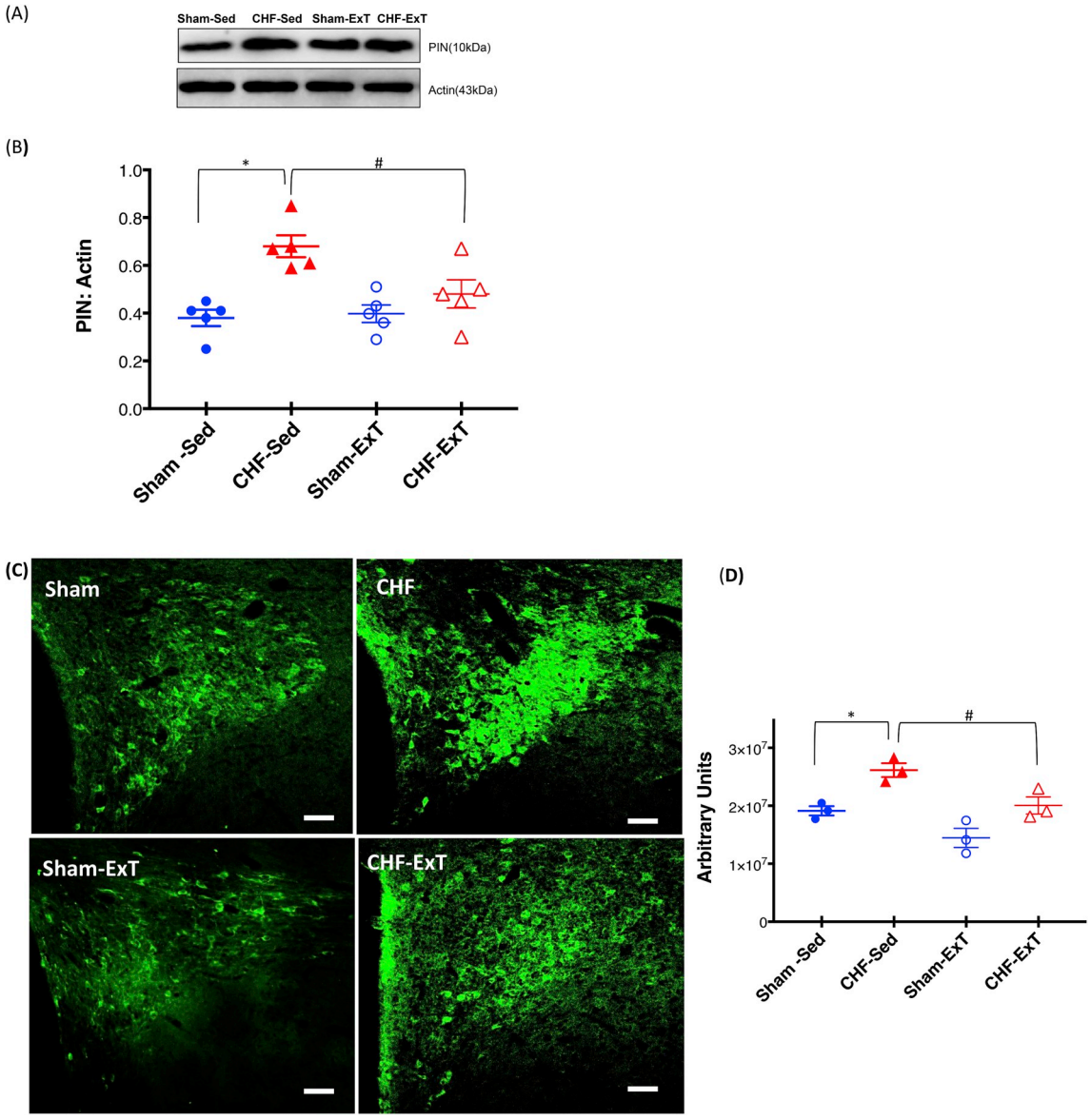

Fig. 3. ExT restores PIN expression in the PVN of CHF. Western blot analysis of PIN in the PVN of four groups of rats: Sham-SED, Sham-ExT, CHF-Sed, and CHF-ExT. (A) Representative Western blot (B) densitometry analyses of PIN level normalized to Actin. Values are mean ± SEM (n = 5 rats per group) *P < 0.05 vs. Sham, #P < 0.05 vs. CHF. (C) Representative Immunofluorescence photomicrographs of the PVN stained for PIN. Green: PIN, Scale bar: 100 μm. (D) Quantification of PIN immunofluorescence staining in the PVN. Values are mean ± SEM (n = 3 rats per group) *P < 0.05 vs. Sham, #P < 0.05 vs. CHF.

from the oxygenase domain of one monomer to the reductase domain of another monomer requiring homodimer formation a prerequisite for catalytic activity of enzyme [47]. BH_4 is required to stabilize the nNOS dimer once it is formed [48,49]. nNOS activation without proper BH_4 binding uncouples standard electron transfer to produce superoxide. Therefore, conditions like BH4 depletion and the addition of a dimerization inhibitor like PIN that favors a change in dimer/monomer ratio of nNOS will affect the proteolytic degradation of nNOS. The nNOS regulation in CHF is not only limited to BH4 availability or PIN overexpression. There are many posttranslational molecular mechanisms like phosphorylation, ubiquitination, sumoylation, etc. are involved in posttranslational regulation and activation of nNOS in the PVN. Previously we have shown that ubiquitination of nNOS is increased in the PVN of CHF rats in AngII-dependent mechanism leading to proteasomal degradation and hence limiting the bioavailability of NO• [21]. In the present study, a relative increase in phosphorylated nNOS-Ser ^{847} suggest another possible mechanism of decrease in nNOS activity and hence limiting the production of NO• in the PVN during CHF.

We used coronary artery ligation model of CHF in our studies which mimics a reliable and consistent simulation of the CHF condition [25–27,45] and advantageous over other models of CHF, such as ventricular pacing. The ligation of the coronary artery simulates the blockage of an artery, commonly seen in patients with CHF. Using this model and three weeks of ExT regimen we have previously shown that ExT can restore the blunted NO• mechanism in the CHF as demonstrated by the restored expression of nNOS [45]. However; the molecular mechanism underlying the beneficial effect of ExT remain to be completely understood. In the present study, we observed decreased PIN protein expression along with a concomitant increase in the nNOS dimer/monomer ratio in the PVN of rats with CHF after ExT. These findings along with the current understanding of PIN function, suggest that the decrease in NO• bioavailability is due to increased PIN expression, which inactivates nNOS via destabilizing dimers and ExT has a beneficial effect via ameliorating the enhanced PIN levels. Silencing of the PIN in neuronal cells resulted in an accumulation of nNOS as well as increase in dimer/monomer ratio with increased NO• production

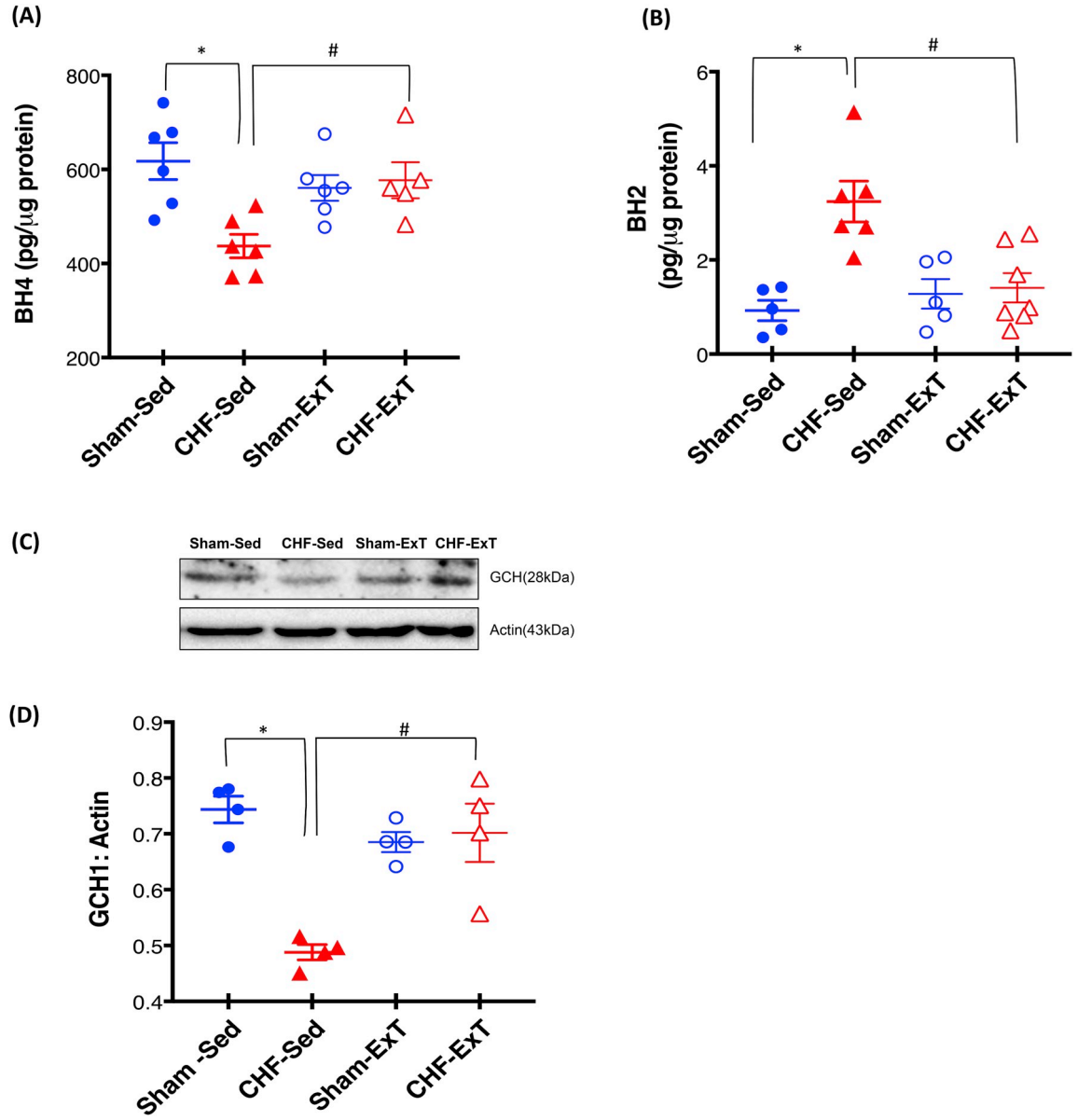

Fig. 4. ExT restores the BH4, BH2 levels and GCH1 expression in the PVN of CHF. (A) BH4 (B) BH2 levels in the PVN lysates measured by ELISA and expressed as per μg of protein. *P < 0.05 vs. Sham, #P < 0.05 vs. CHF Values are mean ± SEM (n = 5–7 rats per group,*P < 0.05) Western blot analysis of GCH1 in the PVN of four groups of rats (C) Representative Western blot (D) densitometry analyses of GCH1 normalized to Actin. Values are mean ± SEM (n = 4 rats per group) *P < 0.05 vs. Sham, #P < 0.05 vs. CHF.

[21], demonstrating that PIN affects nNOS expression and catalytic activity, therefore, plays an essential role in the regulation of nNOS offering a new target for the treatment of CHF and other cardiovascular diseases.

Previously we described that the catalytically active dimeric nNOS [21] as well as that absolute levels of nNOS [20,28], is decreased in CHF. In the current study, we demonstrate that 7-NI-mediated changes in the RSNA are blunted in the CHF suggesting that the nNOS dimerization contributes to the increased sympathoexcitation. 7-NI preferentially (although not exclusively) inhibits nNOS compared with eNOS [50–52] and has been used extensively as a selective inhibitor of nNOS. In the PVN, the relative level of eNOS compared to nNOS, are very low, so we believe that the observed functional changes in CHF are likely due to nNOS. 7-NI binds to substrate binding site and competes with Arginine and BH4, an essential cofactor for nNOS dimer formation and may interfere with dimerization of the enzyme [53].

In this study, we further identified that there is a decrease in the expression of GCH1 leading to decreased PVN levels of BH4 and increased BH2 levels in the CHF which provide yet another possible reason for the uncoupling of nNOS. Therefore, the monomerization of nNOS by dysregulation of intracellular factor involved in dimerization of catalytically active nNOS leads to ubiquitin-mediated proteolytic degradation, and hence a decrease in levels of nNOS in CHF. Interestingly, GCH1 upregulation, as induced by ExT was associated with an increase in BH4 levels and decrease in BH2 levels, and nNOS dimerization suggesting a crucial role of GCH1, and, consequently, BH4 bioavailability, in regulating nNOS activity and coupling. The increased GCH1 expression and hence stabilization of nNOS dimers after ExT is probably by reducing the angiotensinergic mechanisms since ExT has been shown to reduce Ang II levels in CHF [26]. Interestingly Couto GK et al. demonstrated that exercise training causes an increase in GCH1 protein expression which is associated with higher eNOS expression and coupling in coronary arteries of CHF rats [54].

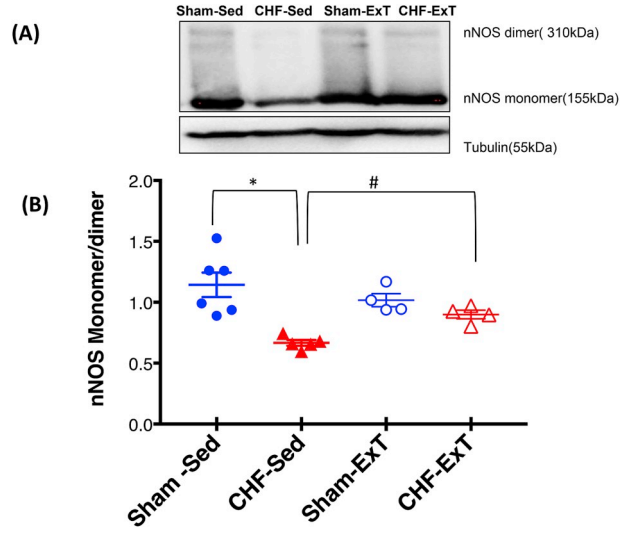

Fig. 5. ExT restores the catalytically active form of nNOS in the PVN of CHF. (A) Estimation of monomers and dimers of nNOS in the PVN of four groups of rats: Sham-SED, Sham-ExT, CHF-Sed, and CHF-ExT. LT-PAGE separated dimeric and monomeric nNOS in cold room and visualized by immunoblotting using an anti-nNOS antibody. (A) Representative LT-PAGE blot (B) densitometry analyses of monomer and dimer protein levels represented as a ratio of dimer to the monomer. Values are mean ± SEM (n = 4–6 rats per group). *P < 0.05 vs. Sham, #P < 0.05 vs. CHF.

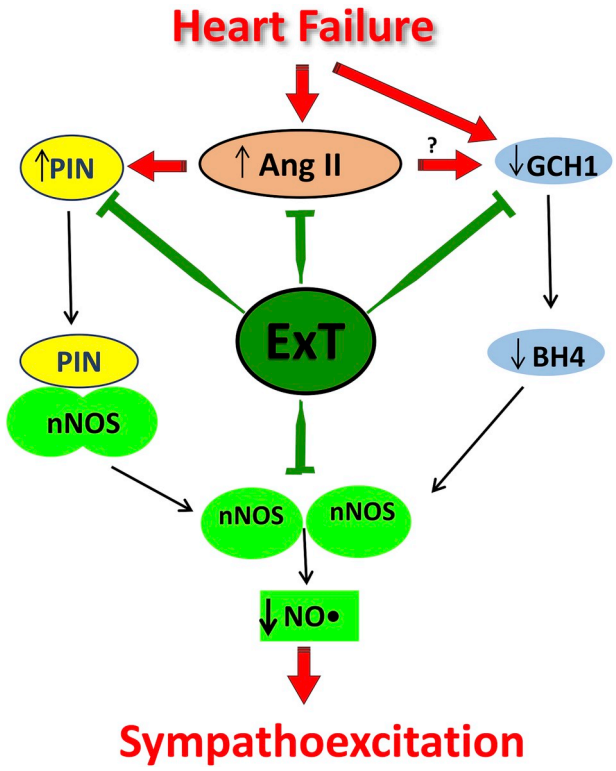

Fig. 6. The proposed molecular mechanism for increased bioavailability of NO• in the PVN after ExT. In CHF, the PIN is over-expressed due to increased Ang II levels and AT_1 receptors in the PVN. Binding of the PIN to nNOS in CHF destabilizes nNOS dimers, which renders nNOS catalytically inactive, either by interfering with the assembly or dimer stability favoring the monomerization. Further reduced GCH1 expression reduces the levels of BH4. This results in decreased catalytically active levels of nNOS in the PVN of CHF rats. A reduced level of nNOS reduces NO• production in the PVN during CHF causing an increase in sympathetic nerve activity. ExT ameliorate the increased PIN levels, decreased GCH1 and BH4 levels as well as decrease the angiotensinogenic mechanism and hence reinstate the active nNOS dimers in the PVN of CHF rats.

The potentiation of angiotensinergic [55] and glutamatergic [56] mechanism within the PVN are associated with CHF, and we have described that ExT normalizes these alterations [26,31]. Previously we have shown that although ExT did not improve cardiac function significantly, however the overall sympathetic drive was attenuated, as indicated by a decrease in excretion of urinary norepinephrine in CHF-ExT group. In this regard, it is of interest to note that CHF patients with lower levels of plasma norepinephrine are given a better prognosis. The present study offers insights into the molecular mechanism at the level of the PVN for the positive effects of ExT during CHF. To date, the mechanisms for the normalization of sympathetic outflow by ExT during CHF have not been elucidated. Here, we found that ExT augments the level of dimeric nNOS, likely through an Ang II-dependent mechanism, since Ang II treatment in NG108 cells enhances PIN expression with a concomitant decrease in nNOS expression, and also there is increased PIN binding to nNOS after Ang II treatment, suggesting a significant functional interaction between these two proteins mediated by Ang II [21]. The possibility that the Ang II-mediated mechanism also regulates GCH1 expression remains to be explored.

Our previous studies have revealed that nNOS in the PVN is regulated post-translationally by nNOS-PIN interactions influenced by Ang II [21] as summarized in Fig. 6. We propose that the expression of the PIN is upregulated, likely due to increased Ang II levels in the PVN in CHF. The binding of the PIN to nNOS leads to the destabilization of nNOS dimers, a conformation required for the catalytic activity of the enzyme. The inactive monomeric state is the trigger that renders nNOS susceptible to ubiquitination and subsequent proteasomal degradation [57]. Reduced active levels of nNOS result in a decrease in the production of NO•, resulting in reduced inhibitory influences to neurons in the PVN, and thereby, enhanced sympathoexcitation observed in CHF. Also, nNOS dimerization without saturating concentration of BH4 uncouples standard electron transfer to produce superoxide. Destruction of NO• by superoxide to form peroxynitrite further limits the bioavailability of NO•. Taken together, these observations provide a significant insight into the possible mechanism(s) within the PVN that contribute to the over-activation of the sympathetic drive during CHF and offer exercise training as a non-pharmacological therapy for treatment of enhanced sympathoexcitation in CHF and other cardiovascular diseases.

Acknowledgments

The work was supported from American Heart Association National Center grant 14SDG19980007(to N. Sharma) and National Institutes of Health, Heart, Lung, & Blood Institute, Grant HL62222(to K.P. Patel).

Appendix A. Supplementary data

Supplementary data to this article can be found online at https://doi.org/10.1016/j.niox.2019.03.005.

Conflicts of interest

The authors declare no potential conflicts of interest.

References

[1] M. Packer, Neurohormonal interactions and adaptations in congestive heart failure, Circulation 77 (1988) 721–730.
[2] AHA, American Heart Association Recommendations for Physical Activity in Adults,

(2017).
[3] L.W. Swanson, P.E. Sawchenko, Paraventricular nucleus: a site for the integration of neuroendocrine and autonomic mechanisms, Neuroendocrinology 31 (1980) 410–417.
[4] H. Kannan, A. Niijima, H. Yamashita, Effects of stimulation of the hypothalamic paraventicular nucleus on blood pressure and renal sympathetic nerve activity, Brain Res. Bull. 20 (1988) 779–783.
[5] K.P. Patel, P.L. Zhang, T.L. Krukoff, Alterations in brain hexokinase activity associated with heart failure in rats, Am. J. Physiol. Regul. Integr. Comp. Physiol. 265 (1993) R923–R928.
[6] A.V. Ferguson, K.J. Latchford, W.K. Samson, The paraventricular nucleus of the hypothalamus - a potential target for integrative treatment of autonomic dysfunction, Expert Opin. Ther. Targets 12 (2008) 717–727.
[7] K.P. Patel, Role of paraventricular nucleus in mediating sympathetic outflow in heart failure, Heart Fail. Rev. 5 (2000) 73–86.
[8] B. Xu, H. Zheng, K.P. Patel, Enhanced activation of RVLM-projecting PVN neurons in rats with chronic heart failure, Am. J. Physiol. Heart Circ. Physiol. 302 (2012) H1700–H1711.
[9] P.E. Sawchenko, L.W. Swanson, The organization and biochemical specificity of afferent projections to the paraventricular and supraoptic nuclei, Prog. Brain Res. 60 (1983) 19–29.
[10] K.P. Patel, P.G. Schmid, Role of the paraventricular nucleus (PVH) in baroreflex-mediated changes in lumbar sympathetic nerve activity and heart rate, J. Auton. Nerv. Syst. 22 (1988) 211–219.
[11] K.G. Commons, D.W. Pfaff, Ultrastructural evidence for enkephalin mediated disinhibition in the ventromedial nucleus of the hypothalamus, J. Chem. Neuroanat. 21 (2001) 53–62.
[12] T. Horn, P.M. Smith, B.E. McLaughlin, L. Bauce, G.S. Marks, Q.J. Pittman, A.V. Ferguson, Nitric oxide actions in paraventricular nucleus: cardiovascular and neurochemical implications, Am. J. Physiol. Regul. Integr. Comp. Physiol. 266 (1994) R306–R313.
[13] R. Jung, M.E. Dibner-Dunlap, M.A. Gilles, M.D. Thames, Cardiorespiratory reflex control in rats with left ventricular dysfunction, Am. J. Physiol. Heart Circ. Physiol. 268 (1995) H218–H225.
[14] K. Zhang, Y.F. Li, K.P. Patel, Reduced endogenous GABA-mediated inhibition in the PVN on renal nerve discharge in rats with heart failure, Am. J. Physiol. 282 (2002) R1006–R1015.
[15] V.C. Biancardi, R.R. Campos, J.E. Stern, Altered balance of gamma-aminobutyric acidergic and glutamatergic afferent inputs in rostral ventrolateral medulla-projecting neurons in the paraventricular nucleus of the hypothalamus of renovascular hypertensive rats, J. Comp. Neurol. 518 (2010) 567–585.
[16] T.L. Krukoff, Central regulation of autonomic function: no brakes? Clin. Exp. Pharmacol. Physiol. 25 (1998) 474–478.
[17] K. Zhang, W.G. Mayhan, K.P. Patel, Nitric oxide within the paraventricular nucleus mediates changes in renal sympathetic nerve activity, Am. J. Physiol. 273 (1997) R864–R872.
[18] K.P. Patel, Y.F. Li, Y. Hirooka, Role of nitric oxide in central sympathetic outflow, Proc. Soc. Exp. Biol. Med. 226 (2001) 814–824.
[19] H. Zheng, X. Liu, Y. Li, N.M. Sharma, K.P. Patel, Gene transfer of neuronal nitric oxide synthase to the paraventricular nucleus reduces the enhanced glutamatergic tone in rats with chronic heart failure, Hypertension 58 (2011) 966–973.
[20] Y.-F. Li, K.P. Patel, Paraventricular nucleus of the hypothalamus and elevated sympathetic activity in heart failure: altered inhibtory mechanisms, Acta Physiol. Scand. 177 (2003) 17–26.
[21] N.M. Sharma, T.L. Llewellyn, H. Zheng, K.P. Patel, Angiotensin II-mediated post-translational modification of nNOS in the PVN of rats with CHF: role for PIN, Am. J. Physiol. Heart Circ. Physiol. 305 (2013) H843–H855.
[22] J.S. Fan, Q. Zhang, M. Li, H. Tochio, T. Yamazaki, M. Shimizu, M. Zhang, Protein inhibitor of neuronal nitric-oxide synthase, PIN, binds to a 17-amino acid residue fragment of the enzyme, J. Biol. Chem. 273 (1998) 33472–33481.
[23] S.R. Jaffrey, S.H. Snyder, PIN: an associated protein inhibitor of neuronal nitric oxide synthase, Science 274 (1996) 774–777.
[24] A.Y. Dunbar, Y. Kamada, G.J. Jenkins, E.R. Lowe, S.S. Billecke, Y. Osawa, Ubiquitination and degradation of neuronal nitric-oxide synthase in vitro: dimer stabilization protects the enzyme from proteolysis, Mol. Pharmacol. 66 (2004) 964–969.
[25] K. Zhang, K.P. Patel, Effect of nitric oxide within the paraventricular nucleus on renal sympathetic nerve discharge:role of GABA, Am. J. Physiol. 275 (1998) R728–R734.
[26] A.C. Kleiber, H. Zheng, H.D. Schultz, J.D. Peuler, K.P. Patel, Exercise training normalizes enhanced glutamate-mediated sympathetic activation from the PVN in heart failure, Am. J. Physiol. Regul. Integr. Comp. Physiol. 294 (2008) R1863–R1872.
[27] A.C. Kleiber, H. Zheng, N.M. Sharma, K.P. Patel, Chronic AT_1 receptor blockade normalizes NMDA-mediated changes in renal sympathetic nerve activity and NR_1 expression within the PVN in rats with heart failure, Am. J. Physiol. Heart Circ. Physiol. 1152 (2010) 1546–1555.
[28] N.M. Sharma, H. Zheng, P.P. Mehta, Y.F. Li, K.P. Patel, Decreased nNOS in the PVN leads to increased sympathoexcitation in chronic heart failure: role for CAPON and Ang II, Cardiovasc. Res. 92 (2011) 342–357.
[29] M.A. Pfeffer, J.M. Pfeffer, M.C. Fishbein, P.J. Fletcher, J. Spadaro, R.A. Kloner, E. Braunwald, Myocardial infarct size and ventricular function in rats, Circ. Res. 44 (1979) 503–512.
[30] M. Palkovits, M. Brownstein, Brain microdissection techniques, in: A.E. Cuello (Ed.), Brain Microdissection Techniques, John Wiley & Sons, Chichester, 1983.
[31] H. Zheng, N.M. Sharma, X. Liu, K.P. Patel, Exercise training normalizes enhanced sympathetic activation from the paraventricular nucleus in chronic heart failure: role of angiotensin II, Am. J. Physiol. Regul. Integr. Comp. Physiol. 303 (2012) R387–R394.
[32] G.C. Vaz, N.M. Sharma, H. Zheng, M.C. Zimmerman, R.S. Santos, F. Frezard, M.A.P. Fontes, K.P. Patel, Liposome-entrapped GABA modulates the expression of nNOS in NG108-15 cells, J. Neurosci. Methods 273 (2016) 55–63.
[33] S. Jurado, L.A. Conlan, E.K. Baker, J.L. Ng, N. Tenis, N.C. Hoch, K. Gleeson, M. Smeets, D. Izon, J. Heierhorst, ATM substrate Chk2-interacting Zn2+ finger (ASCIZ) Is a bi-functional transcriptional activator and feedback sensor in the regulation of dynein light chain (DYNLL1) expression, J. Biol. Chem. 287 (2012) 3156–3164.
[34] K. Mezghenna, J. Leroy, J. Azay-Milhau, D. Tousch, F. Castex, S. Gervais, V. Delgado-Betancourt, R. Gross, A.D. Lajoix, Counteracting neuronal nitric oxide synthase proteasomal degradation improves glucose transport in insulin-resistant skeletal muscle from Zucker fa/fa rats, Diabetologia 57 (2014) 177–186.
[35] S. Choi, J.S. Won, S.L. Carroll, B. Annamalai, I. Singh, A.K. Singh, Pathology of nnos-expressing GABAergic neurons in mouse model of Alzheimer's disease, Neuroscience 384 (2018) 41–53.
[36] E.V.L. Roloff, D. Walas, D.J.A. Moraes, S. Kasparov, J.F.R. Paton, Differences in autonomic innervation to the vertebrobasilar arteries in spontaneously hypertensive and Wistar rats, J. Physiol. 596 (2018) 3505–3529.
[37] Y. Liu, S.L. Baumgardt, J. Fang, Y. Shi, S. Qiao, Z.J. Bosnjak, J. Vasquez-Vivar, Z. Xia, D.C. Warltier, J.R. Kersten, Z.D. Ge, Transgenic overexpression of GTP cyclohydrolase 1 in cardiomyocytes ameliorates post-infarction cardiac remodeling, Sci. Rep. 7 (2017) 3093.
[38] X. Niu, L. Zhao, X. Li, Y. Xue, B. Wang, Z. Lv, J. Chen, D. Sun, Q. Zheng, beta3-Adrenoreceptor stimulation protects against myocardial infarction injury via eNOS and nNOS activation, PLoS One 9 (2014) e98713.
[39] J. Garzon, M. Rodriguez-Munoz, A. Vicente-Sanchez, C. Bailon, R. Martinez-Murillo, P. Sanchez-Blazquez, RGSZ2 binds to the neural nitric oxide synthase PDZ domain to regulate mu-opioid receptor-mediated potentiation of the N-methyl-D-aspartate receptor-calmodulin-dependent protein kinase II pathway, Antioxid. Redox. Signal. 15 (2011) 873–887.
[40] J. Parkash, X. d'Anglemont de Tassigny, N. Bellefontaine, C. Campagne, D. Mazure, V. Buee-Scherrer, V. Prevot, Phosphorylation of N-methyl-D-aspartic acid receptor-associated neuronal nitric oxide synthase depends on estrogens and modulates hypothalamic nitric oxide production during the ovarian cycle, Endocrinology 151 (2010) 2723–2735.
[41] B.M. Ibrahim, A.A. Abdel-Rahman, Enhancement of rostral ventrolateral medulla neuronal nitric-oxide synthase-nitric-oxide signaling mediates the central cannabinoid receptor 1-evoked pressor response in conscious rats, J. Pharmacol. Exp. Ther. 341 (2012) 579–586.
[42] P. Klatt, K. Schmidt, D. Lehner, O. Glatter, H.P. Bachinger, B. Mayer, Structural analysis of porcine brain nitric oxide synthase reveals a role for tetrahydrobiopterin and L-arginine in the formation of an SDS-resistant dimer, EMBO J. 14 (1995) 3687–3695.
[43] Y.F. Li, K.G. Cornish, K.P. Patel, Alteration of NMDA NR1 receptors within the paraventricular nucleus of hypothalamus in rats with heart failure, Circ. Res. 93 (2003) 990–997.
[44] Y.F. Li, W. Wang, W.G. Mayhan, K.P. Patel, Angiotensin-mediated increase in renal sympathetic nerve discharge within the PVN: role of nitric oxide, Am. J. Physiol. Regul. Integr. Comp. Physiol. 290 (2006) R1035–R1043.
[45] H. Zheng, Y.F. Li, K.G. Cornish, I.H. Zucker, K.P. Patel, Exercise training improves endogenous nitric oxide mechanisms within the paraventricular nucleus in rats with heart failure, Am. J. Physiol. Heart Circ. Physiol. 288 (2005) H2332–H2341.
[46] N.M. Sharma, K.P. Patel, Post-translational regulation of neuronal nitric oxide synthase: implications for sympathoexcitatory states, Expert Opin. Ther. Targets 21 (2016) 11–22, https://doi.org/10.1080/14728222.2017.1265505.
[47] W.K. Alderton, C.E. Cooper, R.G. Knowles, Nitric oxide synthases: structure, function and inhibition, Biochem. J. 357 (2001) 593–615.
[48] P. Klatt, S. Pfeiffer, B.M. List, D. Lehner, O. Glatter, H.P. Bachinger, E.R. Werner, K. Schmidt, B. Mayer, Characterization of heme-deficient neuronal nitric-oxide synthase reveals a role for heme in subunit dimerization and binding of the amino acid substrate and tetrahydrobiopterin, J. Biol. Chem. 271 (1996) 7336–7342.
[49] T. Scott-Burden, Regulation of nitric oxide production by tetrahydrobiopterin, Circulation 91 (1995) 248–250.
[50] A. Reiner, Y. Zagvazdin, On the selectivity of 7-nitroindazole as an inhibitor of neuronal nitric oxide synthase, Trends Pharmacol. Sci. 19 (1998) 348–350.
[51] L. Teppema, E. Sarton, A. Dahan, C.N. Olievier, The neuronal nitric oxide synthase inhibitor 7-nitroindazole (7-NI) and morphine act independently on the control of breathing, Br. J. Anaesth. 84 (2000) 190–196.
[52] V.M. da Silva Leal, V.T. Bonassoli, L.M. Soares, H. Milani, R.M.W. de Oliveira,

Depletion of 5 hydroxy-triptamine (5-HT) affects the antidepressant-like effect of neuronal nitric oxide synthase inhibitor in mice, Neurosci. Lett. 656 (2017) 131–137.
[53] A.D. Lajoix, M. Pugniere, F. Roquet, J.C. Mani, S. Dietz, N. Linck, F. Faurie, G. Ribes, P. Petit, R. Gross, Changes in the dimeric state of neuronal nitric oxide synthase affect the kinetics of secretagogue-induced insulin response, Diabetes 53 (2004) 1467–1474.
[54] G.K. Couto, S.M. Paula, I.L. Gomes-Santos, C.E. Negrao, L.V. Rossoni, Exercise training induces eNOS coupling and restores relaxation in coronary arteries of heart failure rats, Am. J. Physiol. Heart Circ. Physiol. 314 (2018) H878–H887.
[55] H. Zheng, Y.-F. Li, W. Wang, K.P. Patel, Enhanced angiotensin-mediated excitation of renal sympathetic nerve activity within the paraventricular nucleus of anesthetized rats with heart failure, Am. J. Physiol. Regul. Integr. Comp. Physiol. 297 (2009) R1364–R1374.
[56] N.M. Sharma, C.J. Cunningham, H. Zheng, X. Liu, K.P. Patel, Hypoxia-inducible factor-1alpha mediates increased sympathoexcitation via glutamatergic N-Methyl-d-Aspartate receptors in the paraventricular nucleus of rats with chronic heart failure, Circ. Heart Fail. 9 (2016).
[57] A.T. Bender, D.R. Demady, Y. Osawa, Ubiquitination of neuronal nitric oxide synthase in vitro and in vivo, J. Biol. Chem. 275 (2000) 17407–17411.